



# Generation and phase noise analysis of a wide optoelectronic oscillator with ultra-high resolution based on stimulated Brillouin scattering

MENGYUE SHI, LILIN YI,\* WEI WEI, AND WEISHENG HU

State Key Lab of Advanced Optical Communication Systems and Networks, Shanghai Institute for Advanced Communication and Data Science, Shanghai Jiao Tong University, Shanghai 200240, China  
\*lilinyi@sjtu.edu.cn

**Abstract:** Microwave signals with broadband tunable frequencies and low phase noise can be widely used in communication systems and radar systems. Optoelectronic oscillators (OEOs) with high Q value have the potential to generate the signals meeting the above requirements. In this paper, we present a simple scheme to realize a widely tunable OEO with ultra-high tuning resolution based on stimulated Brillouin scattering (SBS), meanwhile maintaining the low phase noise for all the generated frequencies. By choosing different high-order sideband of the phase-modulated signal as the SBS pump, the frequency of the generated signal can be widely tuned. The accurate frequency tuning can be achieved by changing the drive signal frequency of the phase modulator. As a result, the obtained signal of the OEO with the frequency tuning range up to 40 GHz, and the tuning resolution as accurate as 10 MHz can be obtained. The influence of the SBS gain and the drive signal on the signal phase noise is analyzed theoretically. The effects of the drive signal and the electrical amplifier on the phase noise of the obtained signal are analyzed experimentally. The results show that the noise figure of the amplifier directly affects the phase noise quality of the acquired signal. And the phase noise of the generated signals is lower than  $-120$  dBc/Hz at 100 kHz offset frequency, which has no relation with the drive signal, or the order of the modulation sideband.

© 2018 Optical Society of America under the terms of the [OSA Open Access Publishing Agreement](#)

**OCIS codes:** (060.0060) Fiber optics and optical communications; (250.0250) Optoelectronics; (290.5900) Scattering, stimulated Brillouin.

## References and links

1. J. Yao, "Microwave photonics," *J. Lightwave Technol.* **27**(3), 314–335 (2009).
2. E. Camargo, *Design of FET Frequency Multipliers and Harmonic Oscillators* (Artech House, 1998).
3. X. S. Yao and L. Maleki, "Converting light into spectrally pure microwave oscillation," *Opt. Lett.* **21**(7), 483–485 (1996).
4. X. S. Yao and L. Maleki, "Optoelectronic oscillator for photonic systems," *IEEE J. Quantum Electron.* **32**(7), 1141–1149 (1996).
5. M. Merklein, B. Stiller, I. V. Kabakova, U. S. Mutugala, K. Vu, S. J. Madden, B. J. Eggleton, and R. Slavik, "Widely tunable, low phase noise microwave source based on a photonic chip," *Opt. Lett.* **41**(20), 4633–4636 (2016).
6. W. C. Swann, E. Baumann, F. R. Giorgetta, and N. R. Newbury, "Microwave generation with low residual phase noise from a femtosecond fiber laser with an intracavity electro-optic modulator," *Opt. Express* **19**(24), 24387–24395 (2011).
7. K. Balakier, M. J. Fice, L. Ponnampalam, A. J. Seeds, and C. C. Renaud, "Monolithically integrated optical phase lock loop for microwave photonics," *J. Lightwave Technol.* **32**(20), 3893–3900 (2014).
8. X. S. Yao and L. Maleki, "Dual microwave and optical oscillator," *Opt. Lett.* **22**(24), 1867–1869 (1997).
9. E. Rubiola, *Phase Noise and Frequency Stability in Oscillators* (Cambridge University, 2008).
10. L. Maleki, "The optoelectronic oscillator," *Nat. Photonics* **5**(12), 728–730 (2011).
11. Z. Xie, S. Li, H. Yan, X. Xiao, X. Zheng, and B. Zhou, "Tunable dual frequency optoelectronic oscillator with low intermodulation based on dual-parallel Mach-Zehnder modulator," *Opt. Express* **24**(26), 30282–30288 (2016).
12. J. Zhang and J. Yao, "Tunable optoelectronic oscillator incorporating a single passband microwave photonic filter," *IEEE Photonics Technol. Lett.* **26**(4), 326–329 (2014).

13. W. Li and J. Yao, "A wideband frequency tunable optoelectronic oscillator incorporating a tunable microwave photonic filter based on phase-modulation to intensity-modulation conversion using a phase-shifted fiber Bragg grating," *IEEE Trans. Microw. Theory Tech.* **60**(6), 1735–1742 (2012).
14. X. Xie, C. Zhang, T. Sun, P. Guo, X. Zhu, L. Zhu, W. Hu, and Z. Chen, "Wideband tunable optoelectronic oscillator based on a phase modulator and a tunable optical filter," *Opt. Lett.* **38**(5), 655–657 (2013).
15. G. P. Agrawal, *Nonlinear fiber optics* (Academic, 2001).
16. S. Preussler and T. Schneider, "Stimulated Brillouin scattering gain bandwidth reduction and applications in microwave photonics and optical signal processing," *Opt. Eng.* **55**(3), 031110 (2015).
17. L. Yi, W. Wei, Y. Jaouën, M. Shi, B. Han, M. Morvan, and W. Hu, "Polarization-independent rectangular microwave photonic filter based on stimulated Brillouin scattering," *J. Lightwave Technol.* **34**(2), 669–675 (2016).
18. M. Shi, L. Yi, W. Wei, G. Pu, and W. Hu, "System performance optimization of frequency-sweeping pump based rectangular Brillouin optical filter," *IEEE Photonics J.* **9**(1), 1–8 (2017).
19. X. S. Yao, "High-quality microwave signal generation by use of Brillouin scattering in optical fibers," *Opt. Lett.* **22**(17), 1329–1331 (1997).
20. B. Yang, X. Jin, H. Chi, X. Zhang, S. Zheng, S. Zou, H. Chen, E. Tangdionga, and T. Koonen, "Optically tunable frequency-doubling Brillouin optoelectronic oscillator with carrier phase-shifted double sideband modulation," *IEEE Photonics Technol. Lett.* **24**(12), 1051–1053 (2012).
21. Y. Qiao, M. Pan, S. Zheng, H. Chi, X. Jin, and X. Zhang, "An electrically tunable frequency-doubling optoelectronic oscillator with operation based on stimulated Brillouin scattering," *J. Opt.* **15**(3), 035406 (2013).
22. H. Peng, C. Zhang, X. Xie, T. Sun, P. Guo, X. Zhu, W. Hu, and Z. Chen, "Tunable DC-60GHz RF generation utilizing a dual-loop optoelectronic oscillator based on stimulated Brillouin scattering," *J. Lightwave Technol.* **33**(13), 2707–2715 (2015).
23. M. Shi, L. Yi, and W. Hu, "SBS-based OEO with high tuning resolution and wide tuning range by selecting different-order phase modulation sideband as pump", in *Optical Fiber Communication Conference (OFC, 2018)*, paper. M1H.4.
24. G. J. Schneider, J. A. Murakowski, C. A. Schuetz, S. Shi, and D. W. Prather, "Radiofrequency signal-generation system with over seven octaves of continuous tuning," *Nat. Photonics* **7**(2), 118–122 (2013).
25. X. S. Yao and L. Maleki, "Multi-loop optoelectronic oscillator," *IEEE J. Quantum Electron.* **36**(1), 79–84 (2000).
26. H. Peng, Y. Xu, X. Peng, X. Zhu, R. Guo, F. Chen, H. Du, Y. Chen, C. Zhang, L. Zhu, W. Hu, and Z. Chen, "Wideband tunable optoelectronic oscillator based on the deamplification of stimulated Brillouin scattering," *Opt. Express* **25**(9), 10287–10305 (2017).
27. W. Shieh and L. Maleki, "Phase noise of optical interference in photonic RF systems," *IEEE Photonics Technol. Lett.* **10**(11), 1617–1619 (1998).

## 1. Introduction

Microwave signals are widely used in radar systems, sensing, signal processing and communication systems [1]. With the development of communication rates and the demand for improved detection resolution of radar systems, new requirements are put forward on the performance of microwave signals, named high frequency, wide tuning range, high resolution, low phase noise and high purity. The traditional microwave signal is generated in the electronic domain, by frequency mixing or multiplication with a low phase noise source [2]. However, the frequency tunability is limited, and the generated signal shows an obvious performance degradation under high frequencies, also suffers from parasitic electromagnetic interferences (EMI).

In the past few decades, microwave photonics provides a new solution for generating microwave signals with high performance [3,4], and even capable of chip-scale integration [5]. Many schemes have been proposed to realize the microwave signal generation in the field of microwave photonics, for example, the optical heterodyne beating of two tones from optical frequency combs (OFCs) [6], or two phase-locked lasers (PLLs) [7]. But it's difficult to filter out the unwanted frequencies. These schemes also usually have complex systems, therefore the cost is high. Optoelectronic oscillators (OEOs) with the potential to generate microwave signal with ultra-low phase noise and flexible tunability is a promising method to satisfy the application requirements [8–10]. The traditional OEO scheme usually introduces an electrical filter in the oscillation loop to select the wanted mode [11]. Though the purity of the generated signal can be guaranteed due to the high suppression ratio of the electrical filter, the tuning bandwidth and accuracy are limited. Microwave photonics filters (MPFs) having the merits of high suppression ratio and large tunability are now widely used in the OEO

scheme for the frequency selection [12–14]. Among these, stimulated Brillouin scattering (SBS) as a common nonlinear effect in the fiber, with the intrinsic advantage of low threshold, narrow bandwidth, flexible frequency adjustment [15,16], has been used to realize MPFs with flexible tunability [17,18] and OEOs with ultra-low phase noise [19]. A carrier phase-shifted double sideband (CPS-DSB) modulation scheme was proposed to realize a frequency-doubling OEO (FD-OEO) based on SBS [20]. The OEO frequency was equal to twice of the SBS frequency shift, and the frequency changing was obtained by tuning the SBS frequency shifting. However, the frequency tuning range of the generated microwave signals is limited to 360 MHz through changing the pump wavelength in a wide range. By intensity-modulation (IM) method to generate an offset frequency to carrier as the SBS pump, the pump frequency can be easily controlled [21]. But the frequency shift directly equals to the frequency of the drive signal of IM, and the frequency tuning range is limited by the drive signal. In order to realize a wider signal tuning range, two lasers are involved as the pump and carrier respectively. In [22], by tuning the pump laser, a microwave signal with a wide tuning range of 40 GHz can be obtained. This scheme requires two high-stable lasers to maintain oscillation. However, the non-correlative frequency drift of the lasers cannot be avoided leading to a phase noise derivation. The tuning resolution in the experiment was 2 GHz limited by the wavelength resolution of the tunable pump laser. Therefore it is difficult to meet the wide-range and high tuning resolution requirements simultaneously, which is a desired feature for an OEO.

In our previous work, a simple scheme to realize a SBS-based OEO with both wide tuning range and high tuning resolution was presented [23]. In this paper, the relationship among the phase noise of the generated OEO frequency, the drive signal, and the high-order modulation sidebands are analyzed in detail. The effect of the electrical amplifier on the phase noise has also been studied carefully. Using one fiber laser as both the SBS pump and the signal carrier, the frequency coherence can be obtained. And a high-order modulation sideband driven by a low-frequency microwave signal is selected for the pump frequency-shifting. Through adjusting the frequency of the drive signal and selecting different-order sidebands of the phase modulated signal as the pump, the frequency tuning range can reach up to 40 GHz, and the frequency tuning resolution can be as accurate as 10 MHz, meanwhile low phase noise for all the generated frequencies was maintained. As a result, the single sideband (SSB) phase noise of all the generated signal is  $-120$  dBc/Hz at 100 kHz offset frequency, which is lower than the phase noise of the drive signal, and has no relationship with the drive signal or the order of the phase modulation sideband.

This paper is organized as follows. In Section 2, the operation principle and theoretical analysis of the widely tunable OEO based on SBS is presented. The system architecture, the phase noise analysis, and the performance of the proposed OEO is introduced in Section 3. Finally, a conclusion is drawn in Section 4.

## 2. Operation principle

The basic operation principle for the SBS-OEO is illustrated in Fig. 1(a). A laser is used as both the SBS pump and the signal carrier. So the phase coherence is maintained. A phase modulator (PM) is usually involved for the phase-to-intensity modulation (PM-IM) conversion, and there is no bias drift to deteriorate the phase noise. Initially, the PM in the OEO loop is seeded by the white noise, then SBS provides a narrow band gain to amplify one of the side modes. When the SBS gain is higher than the threshold of oscillation, OEO oscillates at this particular frequency, which is given by

$$f_{OEO} = |f_p - f_{SBS} - f_c| \quad (1)$$

where  $f_p$  and  $f_c$  is the frequency of the pump and the carrier signal respectively,  $f_{SBS}$  is the Brillouin frequency shift which is 9.65 GHz in the experiment. The frequency tuning of the generated signal is realized by tuning the frequency of the SBS pump.

### 2.1 High-order phase modulation sideband as the pump

Flexible frequency tunability is an important performance for an OEO system. To overcome the limited tuning range of IM, a high-order phase-modulation scheme is adopted. By this way, a comb of sidebands can be generated excited by a high-power sinusoidal reference signal [24]. The single-frequency signal can be expressed as  $f_m$ . When the power of the drive signal is high enough, the spectrum of the phase-modulated signal consists of the carrier components  $f_c$  and the infinite number of harmonics  $f_c \pm nf_m$ . The larger the phase modulation index, the more order of sidebands are excited. By selecting the higher-order sidebands as the pump, the pump frequency can be presented as

$$f_p = f_c \pm nf_m \quad (2)$$

where the - or + denote the left or right sideband of the phase modulation signal in frequency domain. Thus the pump frequency is several times higher than the drive signal, as shown in Fig. 1(a), which provides a widely adjustable frequency offset the carrier [24]. Combining the Eq. (1) and Eq. (2), the frequency of the generated frequency can be shown as

$$f_{OEO} = |\pm nf_m - f_{SBS}| \quad (3)$$

The above frequency is directly determined by the microwave drive signal and the order of the phase modulation sideband, no matter what the carrier frequency is. So a fiber laser with a fixed wavelength is used in the experiment. Through tuning the drive signal frequency and selecting different-order sideband as the pump, the frequency obtained can be finely and coarsely controlled. This solution breaks the frequency adjustment limitation caused by the laser in the traditional SBS-OEO scheme, and improves the frequency tuning flexibility.

### 2.2 Dual-loop structure

In the experiment, the bandwidth of SBS gain is usually about 30 MHz, while the theoretical mode spacing of the loop is  $c/(nL)$ , equaling to several hundred kHz, where  $c$  is the speed of light in the vacuum,  $n$  is the effective refractive index of the medium, and  $L$  is the length of the OEO loop. As a result, lots of longitudinal modes oscillate in a SBS gain bandwidth at the same time. If a dual-loop structure is introduced, the lengths of the two loops in this structure are different, so the corresponding mode intervals are different. Within the Brillouin gain bandwidth, the coincident mode in the two loops is superimposed on each other to gain a higher amplitude, giving priority to oscillation [22, 25]. Through several times oscillations, an amplitude accumulation of the overlapped mode is obtained, while the rest of the mode are suppressed, and then a single mode oscillation is achieved, as shown in Fig. 1(a).

### 2.3 Theoretical analysis of the system phase noise

The phase noises of the OEO system mainly comes from the laser frequency noise via SBS amplification, chromatic dispersion of the fiber, optical interference due to facet reflection, flicker noise of amplifier, thermal noise, shot noise and RIN of the signal laser [26]. The close-in additive phase noise contributed by the laser via SBS in the OEO based on sideband amplification is derived as [26]

$$S_{SBS}(f) = \left[ \frac{\exp(g_p I_p L)}{1 - \exp(g_p I_p L)} \frac{g_p I_p L}{\Delta\nu_B} \right]^2 \cdot [S_s(f) + S_p(f)] \quad (4)$$

where  $g_p$  is the line center Brillouin gain coefficient,  $I_p = P_p / A_{eff}$  is the power intensity of the pump laser,  $P_p$  is the pump power, and  $A_{eff}$  is the effective mode area,  $\Delta\nu_B$  is the gain bandwidth of SBS,  $S_s(f)$  and  $S_p(f)$  are the power spectral density (PSD) of optical frequency noise for the signal laser and pump laser, respectively. In our scheme, the signal laser and the pump laser are coherence, so  $S_p(f)$  can be rewritten as

$$S_p(f) = S_s(f) + nS_m(f) \quad (5)$$

where  $S_m(f)$  is the PSD of optical frequency noise for the drive signal. Usually the noise PSD of the laser is far larger than the noise PSD of the microwave signal, in the order of  $10^4$  or more, and  $n$  cannot reach such a large value, so  $nS_m(f)$  can be ignored. Further, Eq. (4) can be described as

$$S_{SBS}(f) = \left[ \frac{\exp(g_p I_p L)}{1 - \exp(g_p I_p L)} \frac{g_p I_p L}{\Delta\nu_B} \right]^2 \cdot 2S_s(f). \quad (6)$$

In this way, there is no need for two stable lasers with ultra-low phase noise. The noise from the laser also can be converted to the phase noise of the OEO signal through the chromatic dispersion and the reflections of the fiber connectors [27]. So the SSB phase noise of the OEO based on the transfer function model [9, 22] can be obtained as follow [26]

$$S_{OEO}(f) = \left( \frac{FkT + 2qI_{ph}R + N_{rin}I_{ph}^2R}{2P_{OEO}} + \frac{b_{-1}}{f} + S_{SBS}(f) + S_{CD}(f) + S_{interference}(f) + S_{ASE}(f) \right) \cdot |H_{dual-loop}(jf)|^2 \quad (7)$$

where  $F$  is the noise figure of amplifier,  $k$  is the Boltzmann constant,  $T$  is the room temperature,  $q$  is the charge of an electron,  $I_{ph}$  is the photo-current at the output of the photodiode (PD),  $R$  is the load resistance of PD,  $N_{rin}$  is the relative intensity noise (RIN) of the signal laser,  $P_{OEO}$  is the power at the output of PD,  $b_{-1}$  is the flicker noise coefficient of amplifier,  $S_{CD}(f)$  is the additive phase noise induced by the chromatic dispersion,  $S_{interference}(f)$  is the additive phase noise contributed by the laser frequency noise via double reflection process,  $S_{ASE}(f)$  is the amplified spontaneous emission (ASE) noise,  $H_{dual-loop}(jf)$  is the transfer function of the dual-loop OEO. According to the Eq. (4) and Eq. (6), the phase noise influence of the drive signal can be ignored compared to the noise of the laser. Though the phase noise of OEO induced by the laser cannot be improved, this scheme can reduce the number of the lasers, and a stable OEO oscillation condition can be obtained. Through reducing the additive noise of the laser, amplifier and improving the system stability, the phase noise of the OEO system can be reduced.

#### 2.4 SBS induced ASE noise

The ASE noise in the OEO loop mainly comes from the SBS gain, and amplifiers including the optical and electrical amplifier. Under a high pump power, the ASE noise induced by SBS reaches a limit. The corresponding power spectrum of the phase noise can be expressed as [22]

$$S_{SBS\_ASE} = \frac{h\nu_s n_{sp}}{2\eta J_0(\beta) [J_1(\beta)]^2 P_0} \quad (8)$$

where  $h$  is the Plank's constant,  $\nu_s$  is the frequency of Stokes wave,  $n_{sp} \approx \frac{kT}{h\nu_B}$  is the spontaneous emission factor,  $\eta$  is the quantum efficiency of PD,  $\beta$  is the phase modulation index,  $J_0(\beta)$  and  $J_1(\beta)$  are the zeroth-order Bessel function and the first-order Bessel function respectively,  $P_0$  is the optical power at the output of the phase modulator in the OEO loop. From Eq. (8), we can see, when the SBS gain saturates under a high pump power, through improving the phase modulation index and the output power of the phase modulator, the phase noise induced by the ASE noise via SBS can be reduced [22].

### 3. Experimental setup and results

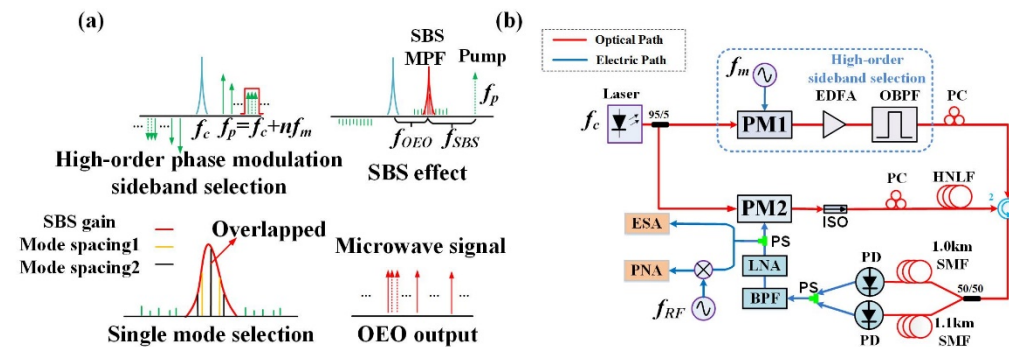


Fig. 1. (a) Operation principle of the frequency tuning using high-order phase modulation sideband as the SBS pump, and the single mode selection by the dual-loop structure. (b) Experimental setup. PM, phase modulator, EDFA, erbium-doped fiber amplifier, OBPF, optical band-pass filter, PC, polarization controller, ISO, isolator, HNLF, high nonlinear fiber, SMF, single mode fiber, PD, photodiode, PS, power splitter, BPF, band-pass filter, LNA, low noise amplifier, ESA, electrical spectrum analyzer, PNA, phase noise analyzer.

The experimental setup to realize the widely tunable SBS-OEO with high resolution is shown in Fig. 1(b). A fiber laser operating at 1551 nm with a power of 16.8 dBm and linewidth of  $\sim 1$  kHz is split into the pump branch and the carrier by a 95:5 optical polarization maintain coupler (PMC). In the pump line, a phase modulator 1 (PM1) with the 3-dB bandwidth of 20 GHz combined with a tunable optical band-pass filter (OBPF) having the minimal 3-dB bandwidth of 15 GHz constitute the frequency control part, where an Erbium-doped fiber amplifier (EDFA) is involved for the power loss compensation, and the output power of the EDFA is about 14 dBm to maintain oscillation. The OBPF is used to select the wanted modulation sideband from the PM1 which is driven by a tunable microwave synthesizer (MS). Through controlling the frequency of the drive signal and the central wavelength of the OBPF, the frequency of the pump can be accurately controlled meanwhile maintains the phase coherence with the carrier. The ASE noise induced by the EDFA also can be reduced by the OBPF. In the carrier branch, a PM2 with the 3-dB bandwidth of 40 GHz is used to realize the electric-to-optic conversion which is modulated by the feedback signal. When the pump signal propagates through the 1-km high nonlinear fiber (HNLF) through a circulator (CIR), a SBS gain is generated from the opposite direction, which is equal to a narrow band-pass MPF. The output signal of the PM2 is amplified when it is located in the SBS gain region. An isolator (ISO) is adopted to remove the back-reflected light, and two polarization controllers (PCs) are used in the two branches to get the maximum SBS gain. Then the output signal from the port 3 of the CIR is separated into two single mode fiber (SMF) links of 1 km and 1.1 km by a 50:50 optical coupler. The outputs of the fiber links are fed into two photodiodes with the 3-dB bandwidth of 40 GHz, separately. Through a 3-dB power splitter (PS), two outputs are coupled together. After being amplified by an electrical low noise

amplifier (LNA), the beating signal of SBS and the signal carrier of PM2 in the dual-loop is send into the PM2 to form the dual-loop OEO architecture. The LNA has the response bandwidth from 100 kHz to 40 GHz with a gain of 30 dB. An electrical band-pass filter (BPF) is needed before the LNA to remove the inevitable harmonics of the beating signal. Finally, the generated microwave signal can be measured in an electrical spectrum analyzer (ESA), and the corresponding phase noise is measured by a phase noise analyzer (PNA).

### 3.1 Flexible frequency tunability

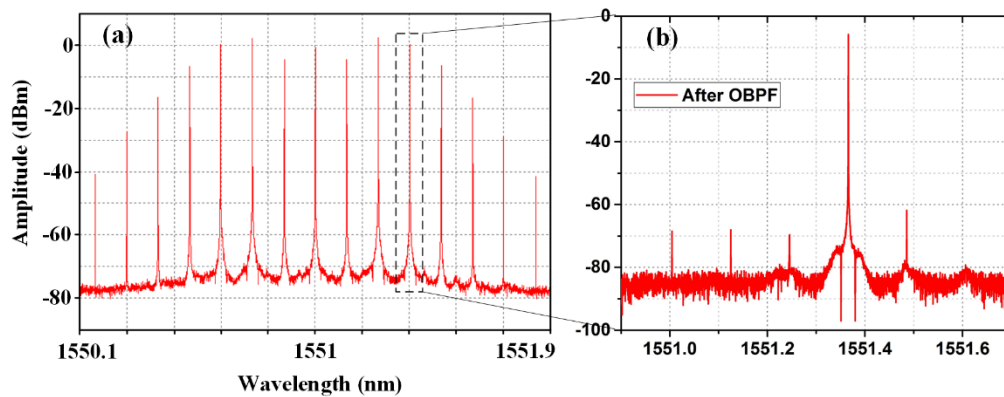


Fig. 2. (a) The optical spectrum of the phase modulated signal. (b) The zoom-in optical spectrum after the OBPF when the 3rd right sideband of the modulated signal is selected.

According to Eq. (3), the frequency of the generated signal is related to the frequency of the drive signal. By selecting the high-order sideband of the phase-modulated signal and adjusting the drive signal, the pump frequency can be coarsely adjusted and finely tuned respectively. And the frequency of the generated microwave signal can be changed correspondingly. In our experiment, the drive signal is firstly set to 15 GHz with a power of 27 dBm by controlling the MS, and 6 modulation sidebands are achieved as shown in Fig. 2(a). The sideband suppression ratio of the OBPF in the experiment is maintained higher than 35 dB. Figure 2(b) is the zoom-in optical spectrum after the OBPF when the 3rd right sideband of the modulated signal is selected. The power of the sideband is lower than the threshold of the SBS gain. So no additional frequency components will be generated. By controlling the central wavelength of the OBPF, the first-order, the second-order and the third-order sideband on the right side of the phase modulation signal is selected as the pump, respectively. Then the microwave signal with the frequency of 5.34 GHz, 20.34 GHz and 35.34 GHz can be obtained, as shown in Fig. 3(a). It can be seen that by selecting different-order phase modulation sidebands under a fixed drive signal, frequency adjustment in a wide frequency range can be realized. So the feasibility to generate high-frequency microwave signal using a low-frequency drive signal is verified. Furthermore, the fine-tuning resolution is as accurate as 10 MHz by tuning the drive signal frequency, as shown in Fig. 3(b), where the obtained frequency is from 4.99 GHz to 5.10 GHz with the tuning step of 10 MHz, and the resolution bandwidth (RBW) of the ESA is set to be 1 MHz. The measured amplitude and phase noise variation in this region is shown in Fig. 4. The insert of Fig. 4 is the zoom-in electrical spectrum of generated OEO signal at the frequency of 5 GHz. As we can see, the amplitude is around 11 dBm, and the phase noise is  $-119$  dBc/Hz at 10 kHz offset frequency. The amplitude floating is smaller than 2 dB, while the side mode suppression ratio (SMSR) is kept higher than 65 dB. So we experimentally verified the effectiveness and feasibility of this scheme to achieve accurate frequency adjustment in high frequency, while the amplitude and phase noise of the obtained frequency maintaining stable.

Theoretically, the tuning accuracy of this scheme is only determined by the drive signal. In fact, due to the instability of the OEO loop, the generated signal will be unstable, which is mainly caused by the frequency drift. So the low-frequency noise of OEO will be very poor, that is, the frequency generated will slowly drift with time. As a result, there will be measurement errors of the measured signal frequency. To avoid this error, the final measured frequency step is 10 MHz. With relatively large tuning steps, the frequency drift caused by the loop instability can be ignored, which ensures the frequency accuracy. Furthermore, a feedback loop is needed to get a higher tuning resolution. When the loop stability is increased, the final tuning accuracy will be greatly increased.

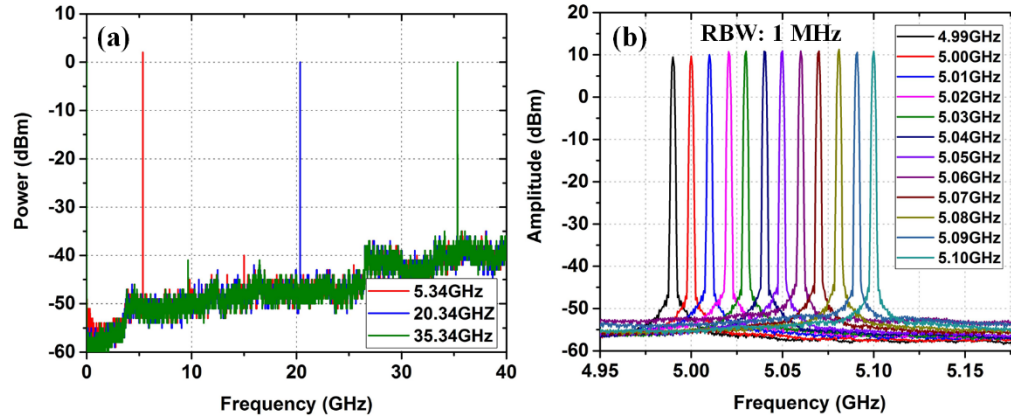


Fig. 3. Frequency tunability of the proposed SBS-OEO. (a) Coarsely OEO frequency tuning by selecting different order phase modulation sideband as the pump with the drive signal of 15 GHz. (b) Finely OEO frequency tuning with the tuning step of 10 MHz.

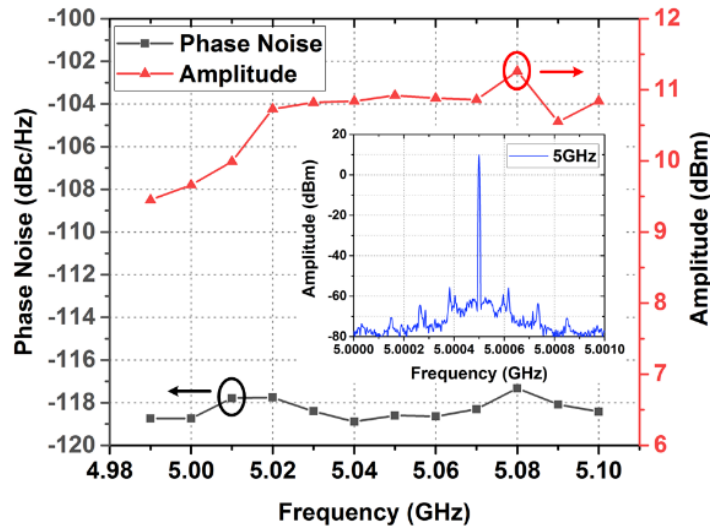


Fig. 4. The measured amplitude and phase noise variation of the obtained frequency from 4.99 GHz to 5.10 GHz with the tuning step of 10 MHz. The insert is the zoom-in electrical spectrum of generated OEO signal at the frequency of 5 GHz.

### 3.2 Phase noise analysis

In section 2, we have theoretically demonstrated that the frequency of the SBS-OEO is determined by the drive signal of the PM. In theory, if the carrier and the high-order modulation sideband beat directly, the frequency obtained will be related to the drive signal,

presenting a  $20[\log(N)]$  phase noise degradation due to the frequency multiplication. It also leads to amplitude deterioration [24]. According to the analysis of the section 2.3, the phase noise of the drive signal is far less than the laser and can be ignored. In this part, we experimentally verify the theory by measuring the phase noise of generated signal under different drive signals with different phase noises. Firstly, a microwave source and a phase-locked loop (PLL) is used to generate a 15GHz signal respectively. The microwave source (MS1) with the relatively poor phase noise is generated by the PLL, In order to magnify the effect, a poor crystal oscillator with 10 MHz output is used as the reference of the PLL. The SSB phase noise is  $-80$  dBc/Hz at 100 kHz offset frequency, as shown in Fig. 5 with black line. The MS2 with the lower phase noise comes from the microwave source, and the SSB phase noise is  $-113$  dBc/Hz at 100 kHz offset frequency, as shown in Fig. 5 with red line. Taking the two 15 GHz signals as the drive signal of PM2 respectively, a 20.34 GHz microwave signal can be obtained by selecting the second-order right side of the phase modulation sideband as a pump, and the corresponding phase noise is shown in Fig. 5. As we can see, they have the similar phase noise curves, and the SSB phase noise is about  $-119$  dBc/Hz at 100 kHz offset frequency, which is better than both of the two drive signals. The phase noise measurement process is carried out at the base-frequency. In the experiment, the OEO frequency down conversion process is achieved by mixing the signal to be measured with a local oscillator signal. A microwave source with ultra-low phase noise is used to generate the local oscillator signal. The phase noise of the local oscillator signal is much lower than the phase noise of the signal to be measured, so the phase noise of the obtained mixed signal is completely determined by the signal to be measured. There will be no phase noise optimization or degradation.

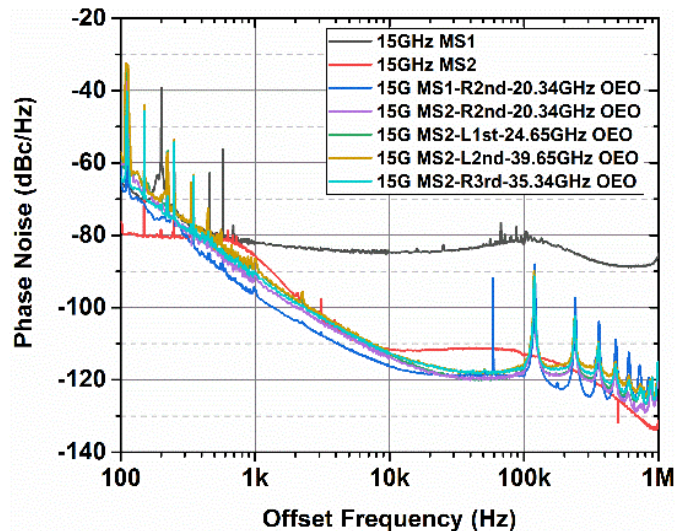


Fig. 5. SSB phase noise of MS1 and MS2 at 15 GHz and the corresponding generated microwave signal at various frequencies with different order phase modulation sideband as the SBS pump.

The effect of the phase modulation sidebands of different orders on the phase noise of the generated signal is also analyzed experimentally. MS2 is used to generate the drive signal with the frequency of 15 GHz. Choosing the 1st, 2nd order left side and the 3rd order right side of the phase modulation sidebands as the pump respectively, the SSB phase noises of the generated microwave signal with the frequency of 24.65 GHz, 39.65 GHz and 35.34 GHz are displayed in Fig. 5. The trends of the phase noise curves under the different phase modulation sidebands are basically the same, and lower than the phase noise of the drive signal. The peak between 50 and 60 kHz of in Fig. 5 is a measurement error, and does not have any phase

noise meaning. So the photonics-based OEO can obtain microwave signal with phase noise lower than the drive signal. Meanwhile, the high order sideband introduces no extra noise as the case in the electrical domain.

Although the phase noise of the drive signal does not affect the noise quality of the resulting OEO signal, the active devices in the loop will introduce additive noise which greatly deteriorates the noise performance of the generated signal, especially the amplifier. The phase noise of three power amplifiers with different noise figure is measured using the scheme described in Fig. 6(a). The phase noise of the mixing signal of two MSs amplified by the three power amplifiers under different frequency are measured with the directly mixing signal as a reference. Figure 6(b) shows the SSB phase noise of different power amplifiers under various frequencies. And the corresponding phase noise of the generated OEO microwave signal under the similar frequency are shown in Fig. 6(b). As can be seen, the noise differences of the amplifiers are consistent with the noise differences of the generated signal. As a result, power amplifier is the main effect leading to the noise difference in different frequencies. Using amplifiers with identical response curves at different frequencies can theoretically reduce this phase noise difference.

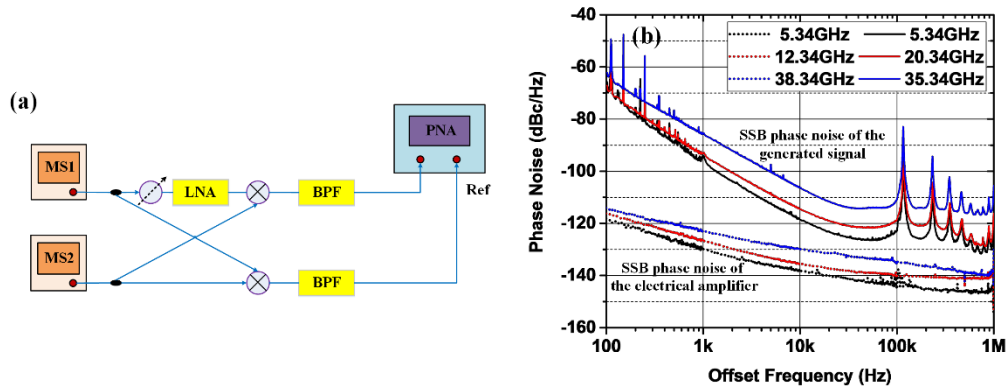


Fig. 6. (a) Structure for measuring the SSB phase noise of the power amplifiers under various frequencies. (b) SSB phase noise of amplifiers and the generated OEO microwave signals at different frequencies.

### 3.3 Performance of the OEO

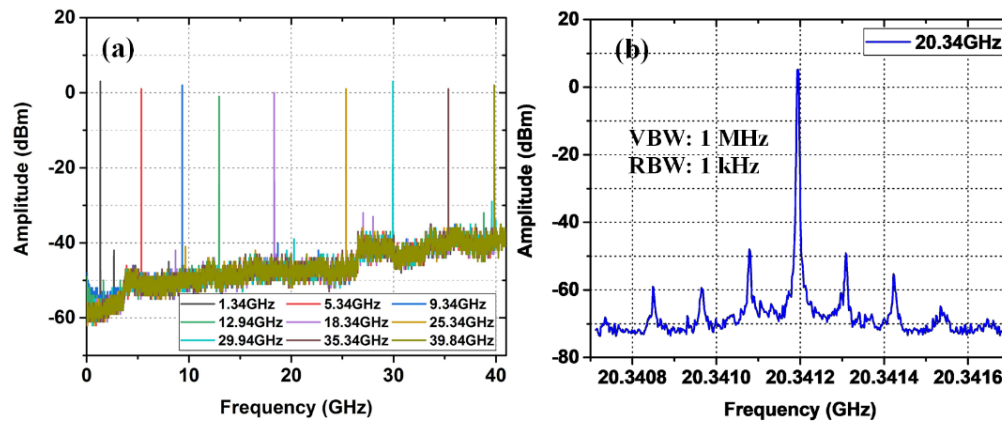


Fig. 7. (a) Electrical spectra of the OEO signal with wide band tuning frequency range up to 40 GHz. (b) The zoom-in electrical spectrum of generated OEO signal under the frequency of 20.34 GHz.

In this part, the wideband frequency tunability, the SMSR, and the phase noise of the generated signal at the frequency tuning range are described in detail. In the experiment, the drive signal is around 10 GHz ~15 GHz to maintain the rejection ratio, and as high as 5th order of sideband has been selected as the pump. Finally the generated microwave signal can reach up to 40 GHz, which is only limited by the devices, such as the modulator, PD and the LNA, as shown in Fig. 7(a). The frequency span in Fig. 7(a) is 40 GHz, and the RBW of ESA is set to be 1 MHz. The spurs in the spectrum are the harmonics, which can be eliminated by filters. An electrical filter with broadband is used in the experiment for removing the inevitable harmonics. And both the purity and the tunability of the generated microwave signal are only determined by the SBS gain. The electrical filter has no effect on the frequency tunability of the OEO. The minimum frequency achieved is related to the minimum drive signal frequency, which is limited by the bandwidth of the optical filter. The minimum frequency of the drive signal is 10 GHz in the experiment to maintain the sideband suppression ratio. When the first order in the right sideband is selected, the pump and the probe carrier has a 10 GHz frequency shifting. For the SBS gain has an about 9.65 GHz frequency shifting offset the pump, the frequency difference between the SBS gain and the carrier is 0.35 GHz, which is the minimum frequency achieved in this scheme. When frequency of the drive signal is 10 GHz, the unwanted phase modulation sideband cannot be removed absolutely limited by the roll-off curves of the optical filter. But the power of the unwanted sideband is much lower than the threshold of the SBS gain. So the unwanted sideband has no effect on the oscillation.

Thanks to the dual-loop structure, the generated signals maintain single mode, and the SMSR reaches higher than 50 dB, as shown in Fig. 7(b), where the observation span is 1 MHz and the RBW is 1 kHz. The corresponding SSB phase noises of the generated signal in the frequency tuning range are shown in Fig. 8. The phase noise curves show a consistency in different frequency, about -120 dBc/Hz at 100 kHz offset frequency. The phase noise difference in low offset frequency comes from the OEO loop jitters, which is induced by the environmental vibration while the difference in high offset frequency comes from the nonlinearity of the active device response, especially the LNA.

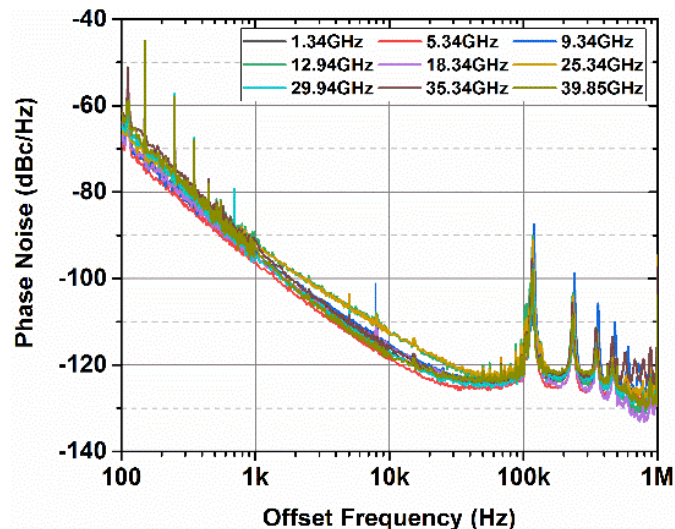


Fig. 8. SSB phase noise of the OEO output signal under various frequencies.

In this scheme, we realized a flexible tuning SBS-OEO, and the frequency can be easily changed by tuning the drive signal. We experimentally demonstrate the relation among the phase noise of the generated microwave signal, the drive signal and the amplifier. The results

reveal that the noise performance is mainly influenced by the amplifier response. And there is no phase noise deterioration with different-order modulation sideband as the SBS pump. If the pump and the carrier signal beat directly without the OEO loop, the theoretical noise deterioration value of additional noise is 6 dB and 9.5 dB when  $N = 2$  and  $N = 3$  respectively. So the performance requirements for the driving signals are reduced. Meanwhile, the upper tuning range in this scheme can be extended to several hundreds of GHz using electrical devices with higher frequency under the higher-order modulation sideband. The frequency tuning resolution is determined by the drive signal of PM1, and is equal to the resolution of the driving signal. Considering the low frequency drift of the generated signals due to loop jitters, the tuning resolution of 10 MHz is chosen to ensure the accuracy of the measured results. Our next work focuses on improving the loop stability to achieve higher frequency tuning accuracy in our scheme. This proposed structure reduces the requirement of using two highly-stable lasers to obtain a low phase noise in the two-laser SBS-OEO structure, and improves the tuning resolution. Also this method extends the tuning range limitation in the traditional single-laser scheme. The generated microwave signal has the advantages of high frequency, flexible tunability and low phase noise, and can be used in radar systems to improve the detecting precision.

#### 4. Summary

In conclusion, we proposed an OEO to generate pure microwave signal with high frequency, wide tuning range, high resolution, and low phase noise based on SBS. Through controlling the order of the phase modulation sideband and the drive signal, flexible frequency tunability up to 40 GHz with the resolution as accurate as 10 MHz can be achieved. The tuning resolution is equal to the resolution of the driving signal. Meanwhile, single mode oscillation is maintained thanks to a dual-loop architecture, and the SMSR is higher than 50 dB in the frequency tuning range. The effects of the drive signal, high-order modulation sidebands, and the amplifier on the phase noise of the generated signal are experimentally analyzed. The results show that the amplifier response is the main factor that aggravates the phase noise. The SSB phase noise of all the generated signal is  $-120$  dBc/Hz at 100 kHz offset frequency, which is independent from the order of the modulation sideband, and even lower than the drive signal. This scheme reduces the requirements of the laser and the driving signal. The tuning range can be broaden to one hundred GHz using higher order sideband and electrical devices with higher frequency while the frequency of the driving signal is maintained low than 15 GHz.

#### Funding

National Natural Science Foundation of China (NSFC) (61575122).